A Monolithic Active Conical Horn Antenna Array for Millimeter and Submillimeter Wave Applications

Vassilis Douvalis, Yang Hao, *Member, IEEE*, and Clive G. Parini, *Member, IEEE*

***Abstract*—In this paper, a novel active integrated conical horn array is presented. Specifically, a 95 GHz quasioptically fed mixer integrated with an annular slot ring antenna was used as the basic element of the proposed active system. For efficient reception, a low cost micro-machined conical horn array was fabricated and placed on the top of active elements. A modified nonorthogonal finite-difference time-domain (FDTD) approach was applied for analyzing the basic conical horn antenna and a hybrid matrix manipulation technique for efficient antenna array modeling. The proposed active conical horn antenna array was fabricated and measured. Numerical simulations have verified the design at its distributed stages presenting very good agreement with the experimental data.**

***Index Terms*—Antennas, array, finite-difference time-domain (FDTD), millimeter wave, submillimeter wave.**

I. Introduction

At millimeter/submillimeter wave frequencies, high-performance and cost effective antenna systems are based on the monolithic active integration [1]. Past attempts to analyze and design integrated horn antenna systems were restricted to the pyramidal horns and to limited numbers of elements [2]–[5]. This is because the numerical methods for the design and verification of such systems are at present very limited. Secondly, constrains on current silicon technology indicate that only pyramidal horns are feasible with a specific flare angle (around 70°) [6].

This paper presents a novel monolithic millimeter wave active conical horn antenna array: A 95 GHz quasioptically fed mixer integrated with an annular slot ring antenna was used as the basic element of the proposed active antenna array. It was fabricated on a very thin silicon substrate to eliminate the substrate modes. For efficient reception, a conical horn antenna array was fabricated using the micro-machining technique and placed on top of the active elements. The conical horn is by virtue of its axial symmetry, capable of handling any polarization of the exciting modes. This new configuration also has less manufacturing difficulties over pyramidal horn array scheme [4]. In this paper we demonstrate a design approach, which includes a conformal finite-difference time-domain (FDTD) technique on single conical horn antenna modeling and the characterization of antenna array using a matrix manipulation technique. Numerical simulations were verified at its distributed stages with experimental data in very good agreement.

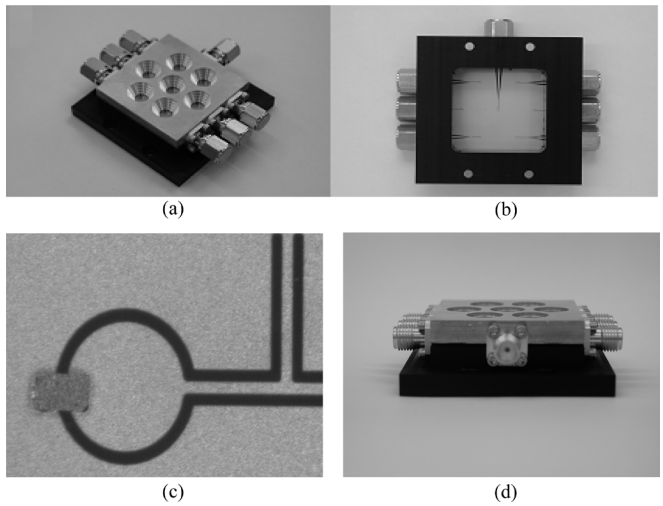

Fig. 1. (a) Fabricated array-front side, (b) back side showing the slot ring array mask, (c) integrated slot ring with diode and filter stub on the mask, (d) side view of the entire structure.

The rest of the paper is organized as follows: Section II presents the structure of the proposed active conical horn antenna array and its design methodology, Section III introduces a novel conformal FDTD technique and a matrix manipulation technique for the conical horn antenna and its array modeling; Section IV presents measurement results for the array and Section V draws conclusions.

II. The Proposed Active Conical Horn Array and Its Design Methodology

The array comprises seven elements arranged at the apexes and the center of a regular hexagon (Fig. 1). It can be separated into two major parts: a conical horn antenna array and a planar quasioptical receiver array. Each element in the receiver array is an integrated annular slot with a single Schottky diode which acts simultaneously both as an antenna and a mixer. The annular slot is chosen for its high symmetrical radiation pattern that is important in quasioptical techniques. Matching circuits and filters in coplanar waveguide line are included to create a receiver at 95 GHz on a Silicon substrate. The conical horn array is placed below the receiver array in the back radiation side of the slot

Manuscript received June 3, 2005; revised November 30, 2005. This work was supported by the Engineering and Physical Sciences Research Council (EPSRC), U.K., under Grant GR/R16945.

V. Douvalis was with the Department of Electronic Engineering, Queen Mary, University of London, London E1 4NS, U.K. He is now with the Greek Army, Athens, Greece.

Y. Hao and C. G. Parini are with the Department of Electronic Engineering, Queen Mary, University of London, London E1 4NS, U.K. (e-mail: y.hao@elec.qmul.ac.uk).

Digital Object Identifier 10.1109/TAP.2006.874338

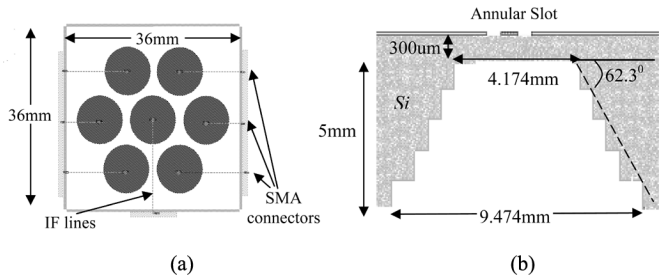

Fig. 2. (a) Top view of proposed conical horn array and (b) side view of a single horn element.

antennas. The purpose of each conical horn is to increase the gain in the signal reception. Since it inserts ideally no losses, it supersedes the lenses that are traditionally used to produce a beam of high Gaussian efficiency [6]. So far, an efficient computer aided design tool that can analyze both passive and active components of a complex millimeter/submillimeter system has not been developed. For example, the traditional FDTD schemes are limited to the Cartesian coordinates only [7]. Therefore when applied in the modeling of conical horn antennas, staircase approximations are needed and hence lead to numerical errors. On the other hand, the nonorthogonal FDTD [8] uses both contravariant and covariant components of vector fields to characterize curved electromagnetic structures. Although the method is accurate over the staircase approximation, it often suffers of late time instability. In addition, numerical simulation of the proposed seven-element conical horn antenna array may result in an insufficient memory error on a typical personal computer. Also, very few efforts have been attempted toward a global analysis technique incorporating both passive and active components [6], [9] and such efforts do not have a general applicability since complexity, time and memory consumption are issues that can be tolerated only when simple active structures are considered.

In this paper, a hybrid approach is proposed to achieve an efficient and accurate design of the proposed active conical horn array. This approach combines the appropriate tools including a local distorted nonorthogonal FDTD algorithm [12], [13] for modeling conical horn antennas. Each aforementioned annular slot is backed with a conical horn for improved reception of the incoming signal. The seven-element array is arranged in a hexagonal form for compactness (Fig. 2). To adapt to the fabrication process (particularly the size of the SMA connectors) the design has allowed for some space between the annular slot rings, which also provides the freedom for extending the length of the horns by quasi-integrating them with flared machined sections [2]. The conical horn is designed to provide an absolute gain of 17 dB. The radius of the horn aperture is calculated at 4.737 mm, the base at 2.087 mm and the flare angle at 27.7° (in stark contrast with the 70° flare angle of a pyramidal horn), which corresponds to a 5-mm high cone.

A hard surface approximation was chosen [Fig. 2(b)] to ease its fabrication on silicon. Furthermore it offers additional advantages over the conventional smooth surface in terms of lower cross-polarization levels and reduced spill over loss [10], [11]. In our design, five sections of circular waveguide with 1 mm height were used to form the 'hard' conical horn antenna.

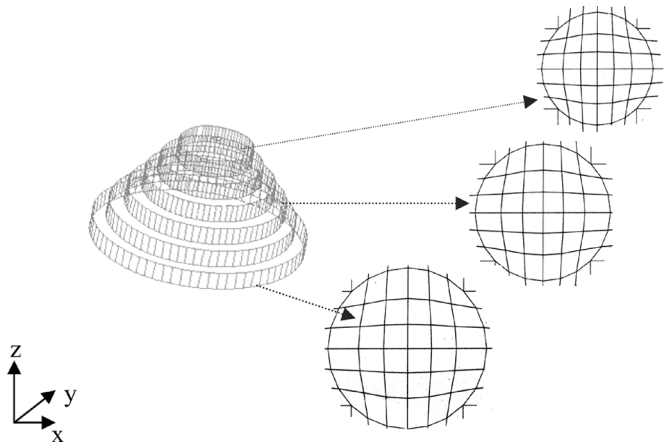

Fig. 3. NFDTD grid for the proposed conical horn as a succession of six circular cross sections.

III. Numerical Modeling of the Conical Horn and the Array

A. Single Element Design

A conformal FDTD scheme based on the local distorted nonorthogonal FDTD (NFDTD) method [8] is used to model the conical horn antennas. The NFDTD algorithm is well suited for the representation of the conical shape and the curvilinear geometry is recorded in the metric tensor

$$g = \begin{pmatrix} g_{xx} & g_{xy} & g_{xz} \\ g_{xy} & g_{yy} & g_{yz} \\ g_{xz} & g_{yz} & g_{zz} \end{pmatrix}. \tag{1}$$

For every curvilinear cell of the nonorthogonal grid, there is a representation similar to (1). The grid is constructed as a succession of circular cross sections of increasing diameter as shown in Figs. 2 and 3. By definition, the metric tensor components in (1) are the scalar products of the local-base vectors in the general grid. At the orthogonal walls of the hard horn the transverse set of vectors $(\vec{x}, \vec{y})$ are at normal angles with the longitudinal direction $\vec{z}$. Therefore at the walls of the horn the metric tensor components in (1) are set as: $g_{xz} = g_{yz} = g_{zx} = g_{zy} = 0$ meaning that the condition of the hard surface is ensured and (1) becomes

$$g = \begin{pmatrix} g_{xx} & g_{xy} & 0 \\ g_{xy} & g_{yy} & 0 \\ 0 & 0 & g_{zz} \end{pmatrix}. \tag{2}$$

To produce results for large time intervals without resorting to lengthy simulations a time subgridding technique is employed [14]: In the orthogonal regions the step is employed [14]: In the orthogonal regions the step is chosen as defined by the Courant criterion $(\Delta t_{\mathrm{orth}})$ while in the nonorthogonal cells the algorithm runs using an integer fraction of the maximum allowed time step $(\Delta t_{\mathrm{curvilinear}})$.

In addition, a NFDTD method was modified to annihilate late time instabilities. It is based on a scheme where only the covariant components are utilized to discretize the Maxwell's equations in the curvilinear system [15]. In this way, there is no need for the traditional interpolation scheme between

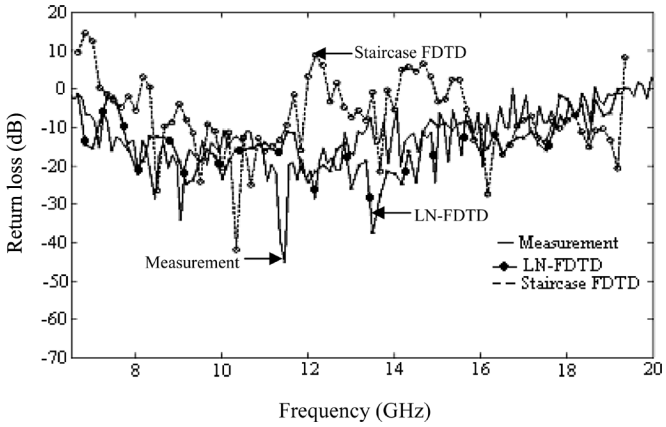

Fig. 4. Comparison of experimental and simulated S_{11}-parameters for a scaled conical horn antenna at microwave frequencies.

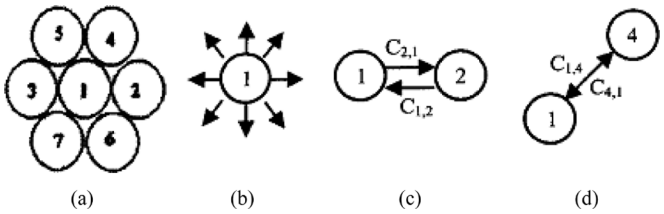

Fig. 5. (a) Array elements, (b) element radiating in free space, (c) and (d) interaction between specific sets of elements used in the matrix manipulation method.

contravariant and covariant components, which is proven to be a source of instabilities [16]. Moreover the abandonment of the contravariant components provides even more computer memory and power utilization. To evaluate the merit of nonorthogonal FDTD over the traditional staircase FDTD in the simulation of conical horn antennas, Fig. 4 is shown. It compares the return loss of a scaled-up model, designed at lower frequencies, of the proposed conical horn antenna. Two simulations have been performed. One uses the LD-NFDTD method (solid dotted line) and another uses the staircase FDTD (dashed line). Both results are compared with measurements (solid line) made in the laboratory. Fig. 4 reveals the reliability and accuracy of the LN-FDTD over the staircase approximation. The latter clearly shows unphysical behavior (positive values of the S_{11} parameters) at some frequencies in the range of 6.5–20 GHz, which result from numerical errors caused by the staircase approximation.

B. Array Design

Since numerically efficient infinite array techniques are not applicable, a new method based on the combination of FDTD algorithm with matrix manipulation techniques is used to predict array performance [17]. It reduces the computational volume to be simulated with FDTD by exploiting the symmetries inherent in any array. Only a small part of the array is analyzed, yielding a matrix description of the coupling and radiation characteristics from which the synthesis of the entire array is going to take place. Specifically, for the proposed conical horn array geometry shown in Fig. 5(a), the decomposed parts to be simulated are shown in Fig. 5(b)–(d). The hexagonal geometry not

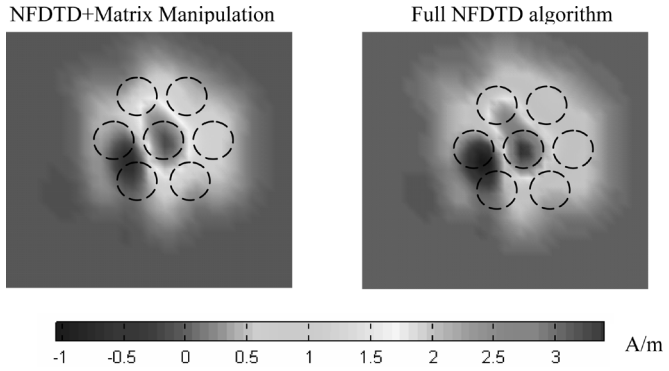

Fig. 6. Time snapshots (H-field) comparison of the array near field computed with a full FDTD simulation and the Matrix method. The matrix method can produce almost the same results with much less computer resources.

only provides compactness but also reduces the generation of grating lobes which otherwise would be present in the array because of the large spacing between the elements. Therefore, the versatility of the array in its radiation characteristics (fixed or scanning beam) is enhanced.

The $C_{i,j}$ components shown in Fig. 5 stand for the coupling interactions between elements stored in the form of a matrix. The radiation matrix obtained from the simulation of Fig. 5(b) is going to reproduce the radiation matrices of all the elements. Also, the scattering matrices of the rest of the elements are going to be produced from the data acquired by the simulations of Fig. 5(c) and (d). This is because:

1) $C_{1,3}$ and $C_{1,5}$ will be the mirror images through the vertical axis of $C_{1,2}$ and $C_{1,4}$ correspondingly.
2) $C_{1,6}$ and $C_{1,7}$ will be the mirror images through the horizontal axis of $C_{1,4}$ and $C_{1,5}$ correspondingly.

The above symmetry properties are carried out by the matrix operators of the matrix manipulation method. Having the radiation and scattering properties of all the elements the array performance can now be evaluated. The methodology is based on the assumption that second neighbors' interaction can be ignored as negligible. This is correct for the specific array, since the high directivity of each horn determined by its aperture size and length will diminish any higher-order couplings as a simple FDTD algorithm run can reveal. Nevertheless the matrix manipulation method can be extended even in cases where this assumption does not apply. Fig. 6 shows the comparison between the full FDTD simulation and the matrix manipulation technique. The time snapshots of the electric field in the near field area of the array are shown for a specific setting (central element radiating in phase and 10.5 dB above the other elements).

IV. Measurement Results and Comparison With Simulation

The fabricated array in different views is shown in Fig. 1 and it radiation patterns were measured at 93 and 95 GHz. In essence, they are obtained from the different values of the generated IF signal as the array is scanned at the E- and H-planes [Fig. 8(a)]. Therefore, these are not the usual antenna pattern measurements but rather active measurements incorporating the operation of the diodes.

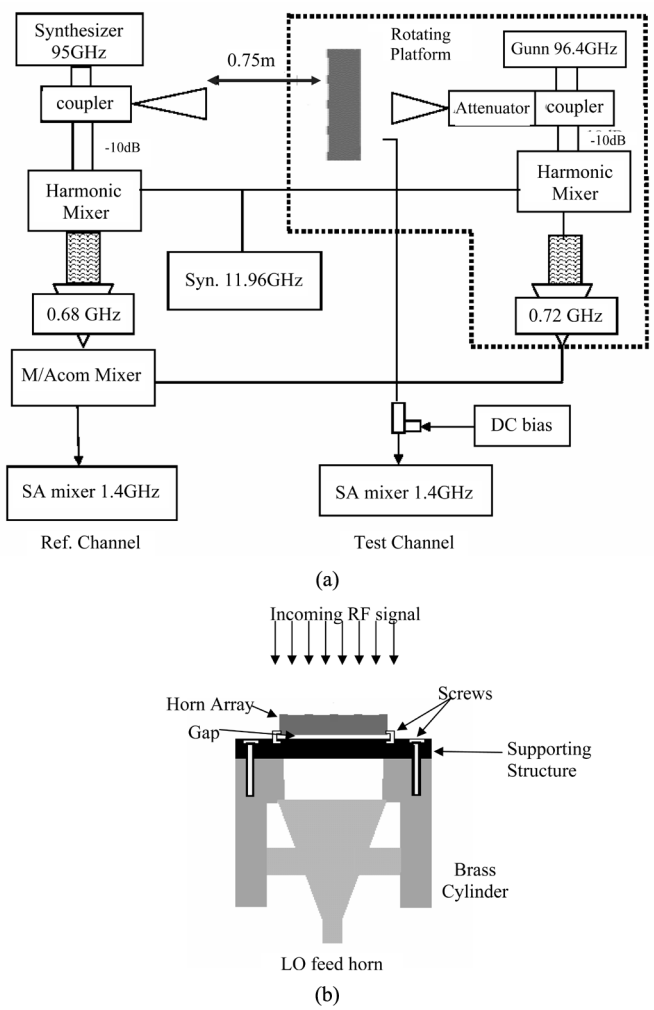

Fig. 7. (a) Radiation pattern measurement set-up at RF 95 GHz and LO 96.4 GHz. (b) Illustration of the set-up at the receiving end.

In all the measurements the diodes were dc biased for optimum performance. Fig. 7 shows the radiation pattern measurement set-up. For the reference channel, the RF at 95 GHz and LO at 96.4 GHz are coupled out from the −10 dB coupler arm and mixed with the 8th harmonics from the synthesizer at 11.96 GHz to obtain frequencies of 0.68 and 0.72 GHz, respectively. These two frequencies are then mixed to obtain a reference IF at 1.4 GHz. Fig. 7(b) shows the horn array and the LO feed system. The RF signal was incident on the side of the horns while the LO radiation was fed from the backside of the array. The mixing process at the diodes is affected primarily by the bias level and secondarily by the level of the LO signal. This means that a low LO signal can be used, without affecting the operation of the mixing diodes, in order to minimize any re-radiation through the horns. This is particularly important if the array is used in a communication system where interference problems should be prevented. A turntable was used to obtain the set of co-polarized and cross-polarized patterns. Measurements were performed at the working frequency of 95 GHz and also at frequencies of 90 and 93 GHz. It must be noted that during the process only one element at a time could be measured. For this reason, the radiation patterns shown include always one element. This either operates alone (the other elements are screened) or in the presence of the array. The 3-dB beamwidth of a single element is around 15°. It is a small value by design, that limits the beam scan of the array but it helps in minimizing the grating lobes, as it will be explained in the conclusion section. A typical IF signal produced as a result of the RF and LO signal mixing from such an element is given in Fig. 8(b). The signal is about 30 dB above the noise floor and it represents a low conversion loss from the proposed active conical horn array. The measured patterns (Figs. 9–11) match the expected/simulation patterns closely. The agreement is better when isolated element operation is considered and worse when the entire array is present. This can be attributed to the simulation of an ideal array in contrast with the real laboratory environment: The necessary surroundings of the array such as coaxial cable connections and supporting structures have not been included in the simulation

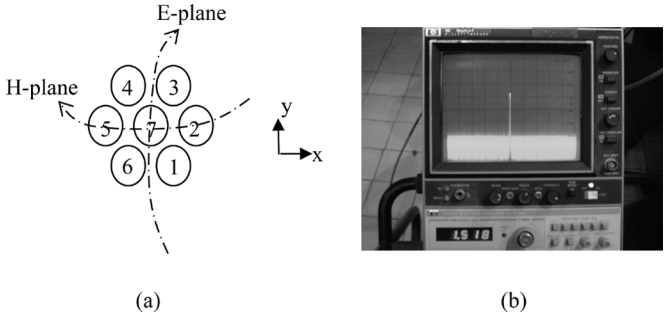

Fig. 8. (a) E- and H-planes of the array, enumeration of the elements and (b) IF signal at 1.518 GHz, 30 dB above noise floor.

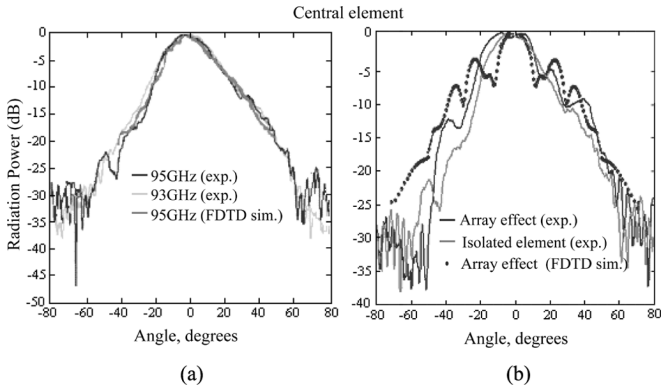

Fig. 9. E-plane patterns for the central element. (a) At different frequencies when isolated and (b) array effect at 95 GHz.

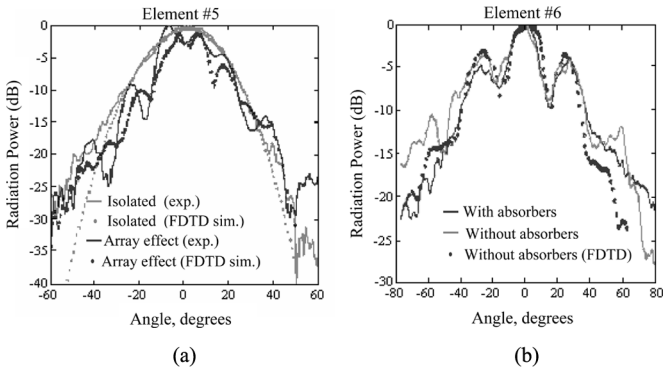

Fig. 10. Patterns at 95 GHz: (a) E-plane patterns for element #5 and (b) H-plane patterns for element #6: the absorbing material smoothes the radiation curve.

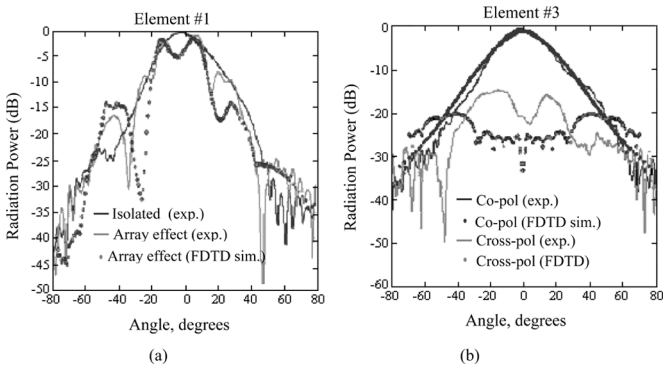

Fig. 11. Patterns at 93 GHz: (a) E-plane patterns for element #1 and (b) E-plane co- and cross-pol for element #3.

model. Even small details that cannot be predicted beforehand (such as the gap created by the screws binding the array to its support structure) permitted the integrated horn antennas to move around two axes so that the E- and H-plane have been proved to have an influence in the radiation pattern.

The effect of mutual coupling due to neighboring elements can also be seen in the figures given. For example, in Fig. 10(a) the coupling effect for the edge element #5 is shown. In Fig. 9 the same effect is depicted for the central element where the neighboring couplings are more. The use of absorber (similar to what is used in an anechoic chamber) placed around the setup is important since it is seen to smooth out the radiation curve significantly [Fig. 10(b)]. There is also a great discrepancy between the measured and simulated cross-polar patterns. The amplitudes of the simulated data are consistently less than the measured ones (at least in the range of 0° to 20°). The high amplitude of the measured cross-polar patterns is attributed to the physical dimensions of the diodes as well as internal reflections/diffractions from the co-polar signal (Fig. 11).

V. Conclusion

A novel monolithic millimeter-wave two-dimensional active conical horn array has been presented as a quasioptical receiver at 95 GHz. The designed resonant frequency was verified by the measurements. The conical horn bears all the assets of other horn types (e.g., directivity, gain, etc.) and moreover predominates, by virtue of its axial symmetry, in the handling of any polarization—especially the circular one. Because of its curved shape, new simulation and fabrication techniques have to be devised and this type of horn element has never before been considered as a part of an integrated system. Conformal FDTD and matrix manipulation techniques combined with commercial software have overcome existing design difficulties. The conformal FDTD algorithm (LD-NFDTD) overcomes the problems set by the traditional FDTD schemes which may be suitable for pyramidal horns but they fail in the simulation of cylindrical ones. The matrix manipulation method provides a fast analysis of the array by exploiting a small part of it in order to predict its overall behavior. Also, the gain and efficiency of the antenna elements is no longer limited by the large horn flare angle of 70°, which is associated with the anisotropic etching of silicon. The achievement of smaller flare angle increases dramatically the freedom of the designer to choose the appropriate size of the horn and to manipulate its radiation characteristics (directivity, gain, mutual coupling with other horns). In addition, the increased directivity (3 dB beamwidth of a single element is at around 15°) that the horns provide reduces to minimum the grating lobe effects that would be present if annular slots were used directly. This is because the inner-element spacing of the *W*-band array is more than three wavelengths. Ordinarily, such sparse spacing leads to strong grating lobes in the pattern if narrow beamwidth elements are not combined with the slots. So, the scan of the array is limited by design to a few degrees, with a strong boresight beam and minimal grating lobes. Pattern measurements at 93 and 95 GHz agree well with the simulation results. The proposed antenna array can be used either for a fixed beam or scanning. Measurements on scanned beam performance need a complex biasing network and results will be presented in future publications. Although conversion losses have not been calculated due to measurement restrictions, the high IF signals are indicative of generally low losses.

Acknowledgment

The authors would like to thank the Engineering and Physical Sciences Research Council (EPSRC), U.K. for the financial support of this project; the reviewers for their valuable comments; Prof. D. Olver for some useful discussions; Dr. B. Alderman, Dr. D. Matheson and Dr. P. Huggard from the Rutherford Appleton Laboratory for the millimeter-wave horn array fabrication and Mr. J. Dupuy for his effort on the millimeter-wave measurements.

References

[1] Y. Qian and T. Itoh, "Progress in active integrated antennas and their applications," *IEEE Trans. Microw. Theory Tech.*, vol. 46, no. 11, pp. 1891–1990, Nov. 1998.

[2] G. M. Rebeiz, L. P. B. Katehi, W. Y. Ali-Ahmad, G. V. Eleftheriades, and C. C. Ling, "Integrated horn antennas for millimeter-wave applications," *IEEE Antennas Propag. Mag.*, vol. 34, pp. 7–16, 1992.

[3] W. Y. Ali-Ahmad, C. C. Ling, and G. M. Rebeiz, "Two-dimensional dual-polarized millimeter-wave horn antenna arrays," in *Proc. Antennas and Propagation Soc. Int. Symp.*, vol. 4, 1990, pp. 1429–1432.

[4] G. V. Eleftheriades and G. M. Rebeiz, "Design and analysis of quasiintegrated horn antennas for millimeter and submillimeter-wave applications," *IEEE Trans. Microw. Theory Tech.*, vol. 41, pp. 954–965, 1993.

[5] ——, "Millimeter-wave integrated diagonal horn antennas," in *Antennas and Propagation Soc. Int. Symp. Digest*, vol. 2, Jun. 1991, pp. 984–986.

[6] S. B. Yeap, M. Rayner, and C. Parini, "Global quasioptical simulations of millimeter-wave receivers," *IEEE Microw. Wireless Comp. Lett.*, vol. 14, pp. 478–480, 2004.

[7] K. S. Yee, "Numerical solution of initial boundary-value problems involving Maxwell's equations in isotropic media," *IEEE Trans. Antennas Propag.*, vol. AP-14, pp. 302–307, May 1966.

[8] R. Holland, "Finite difference solutions of Maxwell's equations in generalized nonorthogonal coordinates," *IEEE Trans. Nucl. Sci.*, vol. NS-30, no. 6, pp. 4591–4689, Dec. 1983.

[9] M. Cryan, S. Helbing, F. Alimenti, P. Mezzanotte, L. Roselli, and R. Sorrentino, "Simulation and measurement of quasioptical multipliers," *IEEE Trans. Microw. Theory Tech.*, vol. 49, no. 3, pp. 451–464, Mar. 2001.

[10] Y. Hao and C. J. Railton, "Analyzing electromagnetic structures with curved boundaries on cartesian FDTD meshes," *IEEE Trans. Microw. Theory Tech.*, vol. 46, no. 1, pp. 82–88, Jan. 1998.

[11] Y. Hao, V. Douvalis, and C. G. Parini, "Modeling conical horn antennas using local distorted nonorthogonal FDTD method," in *Proc. 12th Int. Symp. Antennas*, vol. 1, France, 2002, pp. 67–70.

[12] M. S. Aly and S. F. Mahmoud, "Propagation and radiation behavior of a longitudinally slotted horn with dielectric-filled slots," *Proc. Inst. Elect. Eng. Microwaves, Antennas and Propagation*, vol. 132, pp. 477–479, 1985.
[13] P.-S. Kildal and E. Lier, "Hard horns improve cluster feeds of satellite antennas," *Electron. Lett.*, vol. 24, pp. 491–492, Apr. 1988.
[14] V. Douvalis, Y. Hao, and C. G. Parini, "Reduction of late time instabilities of the finite difference time domain method in curvilinear coordinates," *Proc. Inst. Elect. Eng. Science, Measurement and Technology*, vol. 149, no. 5, pp. 267–272, Sep. 2002.
[15] ——, "A stable nonorthogonal FDTD method," *Electron. Lett.*, vol. 40, pp. 850–851, Jul. 2004.
[16] S. D. Gedney and J. A. Roden, "Numerical stability of nonorthogonal FDTD methods," *IEEE Trans. Antennas Propag.*, vol. 48, no. 2, pp. 231–239, Feb. 2000.
[17] V. Douvalis, Y. Hao, and C. G. Parini, "Fast array analysis using a combination of FDTD with matrix manipulation techniques," *Proc. Inst. Elect. Eng. Microwaves, Antennas and Propagation*, vol. 152, no. 4, pp. 258–264, Aug. 2005.
[18] V. Douvalis and Y. Hao, "A monolithic active conical horn antenna arrays for millimeter and sub-millimeter wave applications," in *Proc. IEEE Antennas Propag. Soc. Int. Symp.*, vol. 1, Jun. 2004, pp. 567–570.

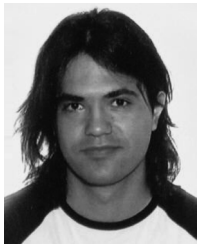

Vassilis Douvalis was born in Athens, Greece, in 1978. He received the B.Sc. and M.Sc. degrees in electrical and electronic engineer from the National Technical University of Athens, in 2000, and the Ph.D. degree in electronic engineering from Queen Mary College, University of London, London, U.K., in 2005. His dissertation was on active antenna arrays.

From 2004 to 2005, he was employed as a Research Assistant on an Engineering and Physical Sciences Research Council (EPSRC), U.K., project concerning photonic antennas and metamaterials. He is currently doing his national service in Greece.

Yang Hao (M'99) received the Ph.D. degree from the Centre for Communications Research (CCR), University of Bristol, Bristol, U.K. in 1998.

From 1998 to 2000, he was a Postdoctoral Research Fellow at the School of Electrical and Electronic Engineering, University of Birmingham, Birmingham, U.K. In May 2000, he joined the Antenna Engineering Group, Queen Mary College, University of London, London, U.K., first as a Lecturer and now a Reader in antenna and electromagnetics. He has co-edited one book, contributed two book chapters, and published over 60 technical papers. His research interests are computational electromagnetics, on-body radio propagations, active integrated antennas, electromagnetic bandgap structures and microwave metamaterials.

Dr. Hao is a Member of the Institution of Electrical Engineers (IEE), London, U.K. He is also a member of Technical Advisory Panel of IEE Antennas and Propagation Professional Network and a member of Wireless Onboard Spacecraft Working Group, ESTEC, ESA. He was a session organizer and Chair for various international conferences and also a keynote speaker at ANTEM 2005, France.

Clive G. Parini (M'96) received the B.Sc.(Eng.) and Ph.D. degrees from Queen Mary College, University of London, London, U.K., in 1973 and 1976, respectively.

He then joined ERA Technology Ltd., U.K., working on the design of microwave feeds and offset reflector antennas. In 1977, he returned to Queen Mary College and is currently Professor of Antenna Engineering and Heads the Communications Research Group. He has published over 100 papers on research topics including array mutual coupling, array beam forming, antenna metrology, microstrip antennas, application of metamaterials, millimeterwave compact antenna test ranges, and millimeterwave integrated antennas.

Prof. Parini is a Fellow of the Institution of Electrical Engineers (IEE), London, U.K. In January 1990, he was one of three co-workers to receive the IEE Measurements Prize for work on near field reflector metrology. He is currently the Chairman of the IEE Antennas and Propagation Professional Network Executive Team and is an Honorary Editor of *IEE Proceedings Microwaves, Antennas and Propagation*. He has been on the organizing committee for a number of international conferences and in 1991 was the Vice Chairman and in 2001 the Chairman of the IEE International Conference on Antennas and Propagation.